Slip along the Hayward fault, California, estimated from space-based synthetic aperture radar interferometry

Roland Bürgmann
Department of Geology, University of California, Davis, California 95616
Eric Fielding
Jet Propulsion Laboratory, California Institute of Technology, 4800 Oak Grove Drive, M.S. 300-233, Pasadena, California 91109
Jai Sukhatme
Department of Geology, University of California, Davis, California 95616

ABSTRACT

For 3–5 years following the 1989 M 7.1 Loma Prieta earthquake, creep along the southern Hayward fault, California, slowed or ceased. Slip apparently resumed pre-earthquake rates by 1994 except for a locked ~3-km-long segment at the southern fault tip, which had consistently slipped at ~9 mm/yr before 1989. We use repeated interferometric synthetic aperture radar (IntSAR) measurements to map active deformation along the Hayward fault while slip rates recovered between 1992 and 1995. If pure strike slip is assumed, then the slip rates estimated from IntSAR range changes between 1992 and 1995 are generally consistent with creepmeter and alignment-array measurements along much of the fault and confirm the temporary locking of the southernmost fault segment. However, along ~6 km of the Fremont segment, IntSAR slip estimates appear to be at least twice those measured in the field. Transient vertical slip (northeast side up) of 2–3 mm/yr near the southern tip of the creep patch could explain this observation. First-order boundary-element models of a vertical frictionless fault in an elastic half-space predict some, but not all, of the inferred vertical slip.

INTRODUCTION

The Hayward fault in the eastern San Francisco Bay area represents a significant seismic hazard in the most densely populated region of northern California. The last major earthquake was the M ~7, 21 October 1868 Hayward fault earthquake that may have extended at depth from Fremont to near Berkeley (Yu and Segall, 1996). No other large historic earthquake has been unequivocally attributed to the Hayward fault, but Williams (1992) documented six southern Hayward fault ruptures during the past 2100 yr. Long-term slip-rate estimates of ~9 mm/yr suggest that more than 1 m of slip potential has accumulated since the most recent event, making the Hayward fault now capable of M >6.5 events (Lienkaemper et al., 1991; Savage and Lisowski, 1992).

Seismic hazard estimates are problematic, however, because the Hayward fault currently exhibits surface creep of 4–9 mm/yr along much of its active trace (Fig. 1). The creep rate has been approximately constant for decades, probably since soon after the 1868 earthquake (Lienkaemper et al., 1991). At the southern end of the recently active fault trace, a 5-km-long fault segment was creeping at a rate close to the long-term slip rate of ~9 mm/yr (Lienkaemper et al., 1991; Koltermann and Gorelick, 1992; Bilham and Whitehead, 1997). For 3–5 years following the 1989 M 7.1 Loma Prieta earthquake, however, creep slowed or ceased on much of the southern Hayward fault (Galehouse, 1997; Lienkaemper et al., 1997). This observation suggests that surface creep along the Hayward fault is sensitive to the regional static stress field in the San Francisco Bay area and varies in response to local events (Simpson and Reasenberg, 1994; Lienkaemper et al., 1997). Existing geodetic data do not yet allow for the discrimination of models of a uniformly creeping or a partially locked Hayward fault (Prescott and Lisowski, 1983; Lienkaemper et al., 1991). Savage and Lisowski (1992) used an idealized friction model to estimate an ~5 km depth of the creeping zone, based on the measured surface creep rate and the average loading rate on the fault. Lack of knowledge about the extent of the locked versus creeping portions of the Hayward fault leads to great uncertainty about potential earthquake magnitudes and probabilities (Lienkaemper et al., 1991; Yu and Segall, 1996).

Interferometric synthetic aperture radar (IntSAR) has the potential to map ground deformation at tens-of-meters resolution over large areas with subcentimeter precision, and promises to significantly improve our ability to image aseismic slip along the Hayward fault. Here we report on IntSAR measurements of active deformation along the Hayward fault spanning a 3.4 yr period from June 1992 to November 1995. We compare our slip estimates with those from creepmeters, fault-crossing alignment arrays, and regional GPS (Global Positioning System) and trilateration measurements.

HAYWARD FAULT SLIP DISTRIBUTION FROM IntSAR

We use synthetic aperture radar (SAR) data collected by the European Space Agency (ESA) ERS-1 spacecraft on 10 June 1992 and 10 November 1995 (ERS Track 70, Frame 2853; orbits 4724 and 22603). We utilize

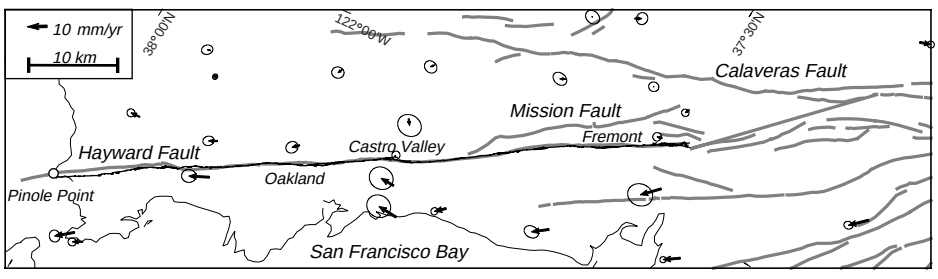

Figure 1. Fault map of eastern San Francisco Bay area in oblique Mercator projection about Pacific plate to Sierra Nevada–Great Valley block Euler rotation pole (Argus and Gordon, 1991). Horizontal lines and vectors are parallel to plate motion. Thin solid line along Hayward fault indicates actively creeping surface trace (Lienkaemper et al., 1991). Also shown are horizontal station velocities determined from combined GPS and geodolite data (Lisowski et al., 1991; Williams, 1995; Murray et al., 1996; Bürgmann et al., 1997).

IntSAR processing techniques developed at the Jet Propulsion Laboratory (Gabriel et al., 1989; Zebker et al., 1994; Peltzer et al., 1996; Rosen et al., 1996) to produce an interferogram from the two SAR images. One phase cycle in the interferogram corresponds to 28 mm of apparent range change between the spacecraft and the Earth's surface. Phase unwrapping yields the total values of the phase difference at each point to produce a contour map of cumulative phase differences (Goldstein et al., 1988). It is not possible to accurately measure the interferometric phase difference in areas (1) that are decorrelated because of too steep topography, (2) where motion exceeding one cycle has occurred across a single pixel, or (3) where significant changes in surface properties have occurred during the time interval between the two SAR images (Zebker and Villasenor, 1992). In our 3.4 yr interferogram of the San Francisco Bay area, we achieve good correlation almost exclusively in urban areas.

Figure 2 shows the unwrapped differential interferogram along the Hayward fault computed from the ERS image pair and corrected for topographic contributions to the apparent range change by using the so-called two-pass method (Gabriel et al., 1989; Massonnet et al., 1993) and 30 m resolution U.S. Geological Survey digital elevation models (DEMs). Apparent range changes in the differential interferogram are due to tectonic deformation of the land surface, combined with atmospheric delay variations and nontectonic land subsidence or rebound. Here we focus on discrete offsets along the Hayward fault that should be little affected by these error sources, which typically have longer wavelengths and lack sharp discontinuities (Goldstein, 1995; Zebker et al., 1997).

Precisely along the trace of the actively creeping Hayward fault (Lienkaemper et al., 1991) we find a sharp phase offset in the interferogram (Fig. 2). This suggests a component of surface fault displacement in the satellite range direction. A scarp along the Hayward fault could produce a range change in the interferogram, if we do not carefully remove topographic effects (Gabriel et al., 1989). However, the U.S. Geological Survey DEMs that we use to remove topographic effects are reported to be accurate at the 7–15 m level, and artifacts remaining from topographic residuals should not exceed ~1 mm of apparent range change (because the ambiguity height of this interferometric pair is about 350 m). Furthermore, the best-determined offsets occur along segments of the Hayward fault in Fremont and Castro Valley that do not have a significant fault scarp associated with them. Offsets near Castro Valley are significantly less than those near Fremont. Analysis of additional interferograms will be needed to show if the fault-parallel edge of an apparent uplift zone to the southwest of the Hayward fault at lat 37.75°, and other features in the image, is caused by atmospheric effects, is related to subsurface water level changes, or is of tectonic nature. Atmospheric delays should not vary sharply across a fault and are not expected to significantly bias our range-step estimates.

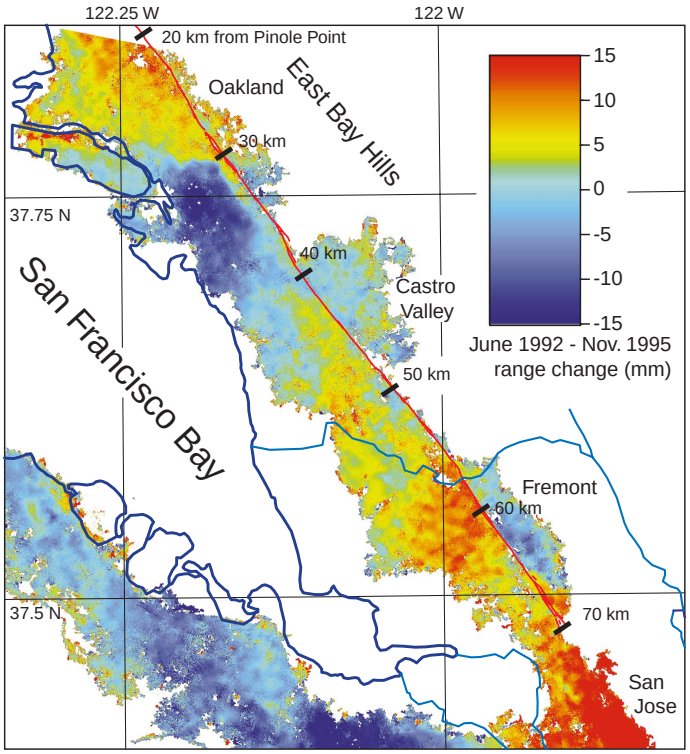

Figure 2. Unwrapped interferogram of two ERS-1 images spanning 3.4 yr period of faulting and strain accumulation near Hayward fault. Range changes are computed from IntSAR interferogram by unwrapping angular phase delays and converting from phase delay to range change. Steep topography and heavy vegetation cause decorrelation leading to loss of range-change information (blank areas). Good correlation occurs almost exclusively in urban areas. An abrupt offset follows trace of recently active strands of Hayward fault indicated by thin red line (Lienkaemper et al., 1991). Black bars along fault mark 10 km distance increments from Pinole Point.

In our analysis, we initially assume that the surface-displacement discontinuity is horizontal and parallel to the N35°W-striking, right-lateral Hayward fault. The ERS-1 descending orbit-track orientation across the San Francisco Bay area is S13.9°W with the radar looking westward. Accordingly, 10 mm/yr of Hayward fault surface creep would produce a range step of 10 mm in a 40 month interferogram, from $\Delta\rho = \Delta\mathbf{d}\cdot\mathbf{e}$, where $\Delta\rho$ and $\Delta\mathbf{d}$ are the range-change and fault-slip vectors, respectively, and $\mathbf{e}$ is the unit vector in the range direction (23° from vertical for ERS, perpendicular to orbital track).

To test the slip rates estimated from the IntSAR data, we compare our results with field measurements of horizontal offset taken previous to and during the observation period (Lienkaemper et al., 1991; Bilham and Whitehead, 1997; Bürgmann et al., 1997; Lienkaemper et al., 1997). Figure 3A shows examples of three fault-crossing range-change profiles along the Hayward fault. Along-fault distances follow Lienkaemper et al.'s (1991) designation with km 0 at Pinole Point where the Hayward fault reaches San Pablo Bay (Fig. 1). Lienkaemper et al. (1997) reported that creep at Camellia Drive (km 66.3) was about 1 mm/yr during our observation period, down from a pre-1989 rate of 9 mm/yr. We also infer <2 mm/yr slip in our SAR interferogram near km 66.3 (Fig. 3A). Near km 63.6, Bilham and Whitehead (1997) measured creep accumulating at 8.5 mm/yr, since early 1994. Here we measure a range offset that would correspond to ~17 mm/yr of strike slip. Alignment arrays established by Galehouse (1997) at km 62.25 and at km 55.65 measured 4.3 mm/yr and ~6 mm/yr creep rates, respectively, between 1992 and 1995 (Lienkaemper, 1997, written commun.). We infer an apparent slip rate of 15 mm/yr at km 62.3, and a rate of 7 mm/yr at km 57.2. GPS measurements at sites several kilometers away from the Hayward fault show displacements of 5–10 mm/yr across the fault (Fig. 1), which are generally consistent with our measurements except for the southernmost 6 km of the fault, where the apparent IntSAR rate exceeds that inferred from GPS data (Bürgmann et al., 1997). However, it is difficult to directly relate the far-field GPS measurements to surface creep rates without further knowledge of the subsurface slip distribution.

We measure the range step from densely spaced, fault-perpendicular profiles to determine an offset distribution profile along the Hayward fault (Fig. 3B). Along extended stretches of the fault, no slip estimates are possible owing to signal decorrelation just to the east of the Hayward fault. Figure 3B compares the historic creep measurements averaged over several decades (Lienkaemper et al., 1991) with rates measured with creepmeters and alignment arrays during the 1992–1995 period (Bilham and Whitehead, 1997; Lienkaemper et al., 1997), and those estimated from the 1992–1995 IntSAR data. IntSAR slip-rate estimates and field measurements agree within 3–5 mm/yr along the Hayward fault as far south as km 58. There is a reduction in slip rate estimated from IntSAR between km 40 and km 44. However, along the southernmost 5–7 km, the IntSAR

apparent-creep-rate estimates are about twice those measured in the field. Below, we suggest that this discrepancy is due to transient vertical slip near the fault tip of the Hayward fault.

DISCUSSION

Large discrepancies between creep-rate estimates from the IntSAR range measurements and those from field observations may have several causes. The deficit between field measurements and the IntSAR slip estimates could partly be due to the limited width (5–100 m) of the field-based measurements, if fault offsets are distributed over a greater width. Some fault-crossing profiles in our data appear to accumulate the total offset across 2–3 pixel widths, where each pixel is ~80 m wide (Fig. 3A). However, such accumulation would imply that the pre-1989 slip measurements are underestimates by a similar factor and that the Hayward fault consistently slips at >10 mm/yr along its southern end. This value exceeds its estimated geologic rate. Because our estimates along the parts of the fault northwest of Fremont agree quite well with those determined from field observations, we do not think the discrepancy can be easily explained by incomplete sampling of fault creep in field measurements. The distributed appearance of the range change in some profiles is likely to be caused by smoothing from filters applied to the data.

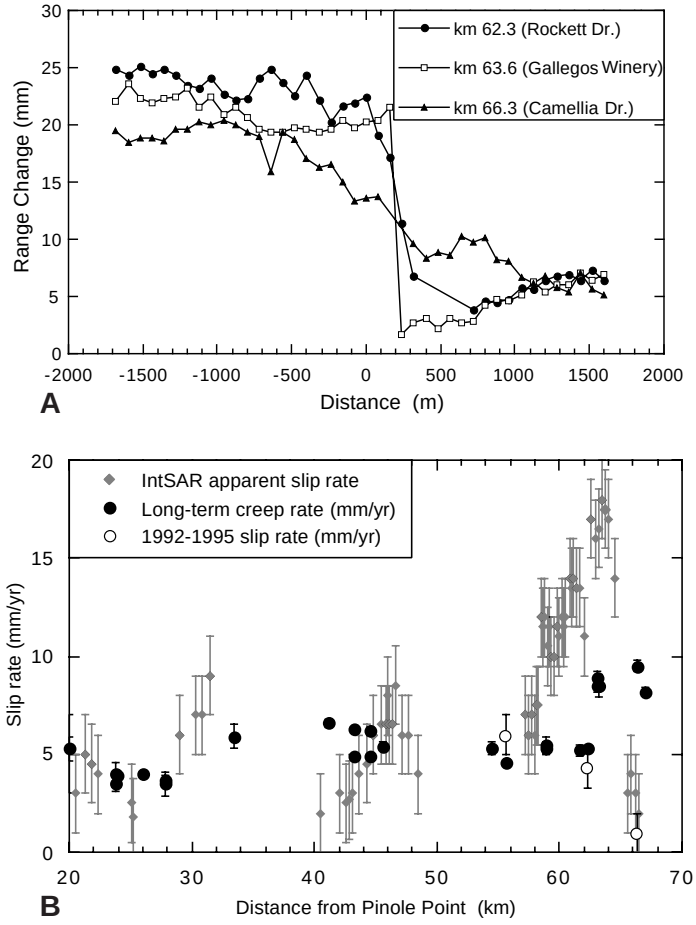

Figure 3. A: Fault-crossing range-change profiles across Hayward fault. Labels in key indicate distance in kilometers from Pinole Point (Fig. 1). Field measurements during IntSAR data interval were taken at km 62.25, km 63.6, and km 66.3. B: Creep-rate distribution along Hayward fault. Solid circles—historic measurements (curb offsets, alignment arrays, etc.) by Lienkaemper et al. (1991). Open circles—alignment array and creepmeter measurements from 1992 to 1995 (Bilham and Whitehead, 1997; Lienkaemper et al., 1997; Lienkaemper, 1997, written commun.). Gray diamonds—creep rates from 1992–1995 IntSAR range offsets assuming horizontal strike slip.

The southern San Francisco Bay area has exhibited significant vertical motion due to the withdrawal and recharge of ground water (Poland and Ireland, 1988). Where the Hayward fault crosses the Alameda fan, differential vertical motion may be the result of differential compaction or expansion where the fault separates an ~250-m-thick fan complex to the southwest from thinly covered bedrock to the northeast (Koltermann and Gorelick, 1992). However, aquifers throughout the region apparently rebounded by up to 6 cm in the time period covered by our interferogram (Fielding et al., 1997). Aquifer rebound would produce a southwest-up offset, opposite to that needed to enhance fault-slip estimates.

Strike-slip faulting along the Hayward fault may be accompanied by a vertical slip component that projects into the range measurement by a factor of the cosine of the incidence angle of ~23°. If a mean slip rate of 8 mm/yr as observed near km 63.7 (Bilham and Whitehead, 1997) is assumed, this possibility requires that the northeast block is being upthrown at 2–3 mm/yr to produce the ostensible 15–18 mm/yr pure-horizontal-creep rate estimate. As there is no well-developed fault scarp along this part of the Hayward fault, and Quaternary vertical-slip rates are <0.5 mm/yr near Fremont (Koltermann and Gorelick, 1992), any vertical creep must be a transient feature. Because field observations only measure horizontal strike slip, we can combine them with the IntSAR data to gain new knowledge about the vertical slip component along the Hayward fault. Without the complementary field observations, the IntSAR data could very easily have been misinterpreted as indicating very high strike-slip rates.

Transient vertical slip could be caused by complex slip distributions near the tips of a creeping fault. We utilize boundary-element models (Thomas, 1993) with zero-traction boundary conditions along a 60-km-long, 5-km-deep, vertical fault. The model fault is discretized into 1-km-long and 0.5-km-wide fault segments. The fault is embedded in a homogeneous, isotropic half-space and is loaded by a buried strike-slip dislocation representing interseismic shear at 40 mm/yr below 15 km depth. Near the tip of the creeping fault, we find vertical slip at the surface. Whereas strike slip follows an approximately elliptical distribution with a maximum slip rate of ~8 mm/yr (not shown), dip slip increases toward the fault ends with opposite signs at either end. At the southeastern end of the fault, vertical slip is northeast up, thereby enhancing the offset in the radar range direction (Fig. 4).

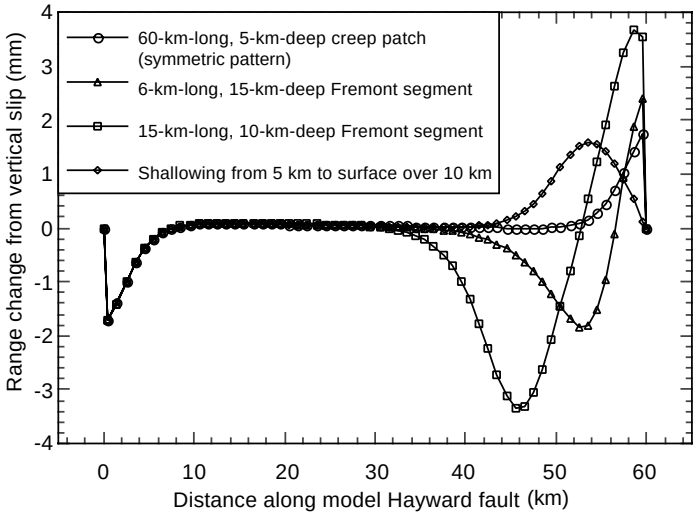

Figure 4. Predicted 1992–1995 range changes from vertical slip of surface elements along simple boundary-element model. All models consist of vertical frictionless strike-slip fault embedded in elastic half-space and loaded by a strike-slip dislocation slipping at 40 mm/yr below 15 km depth. In addition to rectangular, 60 × 5 km geometry, we evaluate effects of varying depth along southernmost part of fault, as indicated in legend.

The model dip-slip rate of ~0.6 mm/yr near the tip of the 5 × 60 km model fault does not reconcile the observed discrepancy. Thus, we evaluate slip distributions of somewhat more complex geometries, focusing on the effect of a deeper-slipping Fremont segment and that of a shallowing slip patch as the southeast fault tip is approached. Figure 4 shows the added range change predicted in our interferogram from these geometric effects. Vertical slip caused by a 10-km-deep, 15-km-long Fremont segment would increase the range observation almost 4 mm in the southernmost 5 km, and decrease the range offset by a similar amount over an adjoining ~10-km-long segment. However, this model also predicts as much as 10 mm/yr strike slip along the southern fault segment, which agrees with pre–Loma Prieta estimates, but not with field measurements during our experiment. Linear shallowing of the creeping patch along the southeasternmost 10 km of the Hayward fault causes a broad increase of range offset by ~2 mm. We tentatively suggest that slip may have recommenced at shallow levels and not yet propagated to greater depths in the 1992–1995 interval, explaining the low strike-slip rates and some of the inferred vertical slip.

Dip slip could be further enhanced if the fault is not vertical (Bilham and Whitehead, 1997), if frictional parameters vary along the fault, or if the applied tractions are not horizontal and are in response to a spatially heterogeneous stress field. Loading and slip of the southern Hayward fault may be particularly affected by interaction with the nearby Mission and Calaveras faults, or by the effects from the coseismic and postseismic stress fields of the Loma Prieta earthquake (Simpson and Reasenberg, 1994; Bürgmann et al., 1997). For example, Simpson and Reasenberg (1994) found that if the Hayward fault is off vertical, significant up-dip stresses would have resulted from the Loma Prieta earthquake.

CONCLUSIONS

Interferograms of SAR images collected in 1992 and 1995 reveal sharp offsets along the Hayward fault that are due to aseismic strike slip and dip slip. Slip rates derived from the IntSAR data assuming pure strike-slip faulting exceed ground-based slip measurements along the southern Fremont segment. We suggest that a transient vertical-slip component is responsible for this discrepancy. The dip-slip component must be transient, because geologic long-term dip-slip estimates along the southern Hayward fault are much smaller than those inferred. Some of the vertical slip is a natural result of horizontal loading of a shallow strike-slip fault (Fig. 4). The magnitude of dip slip is sensitive to details of the subsurface fault geometry, frictional parameters, and the tractions on the fault. SAR interferometry, in combination with ground observations, promises to significantly improve our understanding of the mechanics of shallowly creeping faults. Future analysis of a large number of interferograms in combination with complementary GPS and creepmeter observations will allow us a view of the active deformation along the Hayward fault at an unparalleled spatial and temporal resolution.

ACKNOWLEDGMENTS

We thank Jim Lienkaemper for providing us with the precise Hayward fault trace coordinates and recent creep-rate measurements. We appreciate discussions with Paul Segall, Jim Lienkaemper, Howard Zebker, Falk Amelung, and Gilles Peltzer. Mark Murray compiled and combined the GPS data shown in Figure 1. James J. Lienkaemper, James C. Savage, and Joann M. Stock provided very helpful reviews. We thank David Pollard for providing the boundary-element modeling code. European Space Agency ERS-1 data were acquired from Radarsat International. Financially supported by National Science Foundation grant EAR-9706374 and U.S. Geological Survey National Earthquake Hazard Reduction Program grant 1434-96-G-2744 to Bürgmann.

REFERENCES CITED

Argus, D. F., and Gordon, R. G., 1991, Current Sierra Nevada–North America motion from very long baseline interferometry; implications for the kinematics of the western United States: Geology, v. 19, p. 1085–1088.

Bilham, R., and Whitehead, S., 1997, Subsurface creep on the Hayward fault, Fremont, California: Geophysical Research Letters, v. 24, p. 1307–1310.

Bürgmann, R., Segall, P., Lisowski, M., and Svarc, J., 1997, Postseismic strain following the 1989 Loma Prieta earthquake from GPS and leveling measurements: Journal of Geophysical Research, v. 102, p. 4933–4955.

Fielding, E. J., Blom, R. G., Evans, D. L., and Bürgmann, R., 1997, Distinguishing ground subsidence due to subsurface material removal from vertical tectonic motions with SAR interferometry: Eos (Transactions, American Geophysical Union), v. 78, p. 141.

Gabriel, A. K., Goldstein, R. M., and Zebker, H. A., 1989, Mapping small elevation changes over large areas—Differential radar interferometry: Journal of Geophysical Research, v. 94, p. 9183–9191.

Galehouse, J. S., 1997, Effect of the Loma Prieta earthquake on fault creep rates in the San Francisco Bay region: U.S. Geological Survey Professional Paper 1550-D, p. 193–207.

Goldstein, R., 1995, Atmospheric limitations to repeat-track radar interferometry: Geophysical Research Letters, v. 22, p. 2517–2520.

Goldstein, R. M., Zebker, H. A., and Werner, C. L., 1988, Satellite radar interferometry—Two-dimensional phase unwrapping: Radio Science, v. 23, p. 713–720.

Koltermann, C. E., and Gorelick, S. M., 1992, Paleoclimatic signature in terrestrial flood deposits: Science, v. 256, p. 1775–1782.

Lienkaemper, J. J., Borchardt, G., and Lisowski, M., 1991, Historic creep rate and potential for seismic slip along the Hayward fault, California: Journal of Geophysical Research, v. 96, p. 18261–18283.

Lienkaemper, J. J., Galehouse, J. S., and Simpson, R. W., 1997, Creep response of the Hayward fault to stress changes caused by the Loma Prieta earthquake: Science, v. 276, p. 2014–2016.

Lisowski, M., Savage, J. C., and Prescott, W. H., 1991, The velocity field along the San Andreas fault in central and southern California: Journal of Geophysical Research, v. 96, p. 8369–8389.

Massonnet, D., Rossi, M., Carmona, C., Adragna, F., Peltzer, G., Feigl, K., and Rabaute, T., 1993, The displacement field of the Landers earthquake mapped by radar interferometry: Nature, v. 364, p. 138–142.

Murray, M. H., Segall, P., Prescott, W. H., King, N. E., Lisowski, M., Bürgmann, R., Freymueller, J. T., Williams, S. D. P., and Romanowicz, B., 1996, The deformation field across the Pacific–North America plate boundary in northern California from EDM, GPS, and VLBI observations: Eos (Transactions, American Geophysical Union), v. 77, p. 143.

Peltzer, G., Rosen, P., Rogez, F., and Hudnut, K., 1996, Postseismic rebound in fault step-overs caused by pore fluid flow: Science, v. 273, p. 1202–1204.

Poland, J. F., and Ireland, R. L., 1988, Land subsidence in the Santa Clara Valley, California, as of 1982: U.S. Geological Survey Professional Paper 497F, p. 1–46.

Prescott, W. H., and Lisowski, M., 1983, Strain accumulation along the San Andreas fault system east of San Francisco Bay, California: Tectonophysics, v. 97, p. 41–56.

Rosen, P. A., Hensley, S., Zebker, H. A., Webb, F. H., and Fielding, E. J., 1996, Surface deformation and coherence measurements of Kilauea Volcano, Hawaii, from SIR-C radar interferometry: Journal of Geophysical Research, v. 101, p. 23109–23125.

Savage, J. C., and Lisowski, M., 1992, Inferred depth of creep on the Hayward fault, central California: Journal of Geophysical Research, v. 98, p. 787–795.

Simpson, R. W., and Reasenberg, P. A., 1994, Earthquake-induced static-stress changes on central California faults: U.S. Geological Survey Professional Paper 1550-F, p. 55–89.

Thomas, A. L., 1993, Poly3D: A three-dimensional, polygonal element, displacement discontinuity boundary element computer program with applications to fractures, faults, and cavities in the Earth's crust [Master's thesis]: Stanford, California, Stanford University, 221 p.

Williams, P. L., 1992, Geologic record of southern Hayward fault earthquakes: California Division of Mines and Geology Special Publication, v. 113, p. 171–179.

Williams, S. D. P., 1995, Current motion on faults of the San Andreas system in central California inferred from recent GPS and terrestrial survey measurements [Ph.D. thesis]: Durham, England, University of Durham, 293 p.

Yu, E., and Segall, P., 1996, Slip in the 1868 Hayward earthquake from the analysis of historical triangulation data: Journal of Geophysical Research, v. 101, p. 16101–16118.

Zebker, H. A., and Villasenor, J., 1992, Decorrelation in interferometric radar echoes: IEEE Transactions on Geoscience and Remote Sensing, v. 30, p. 950–959.

Zebker, H. A., Rosen, P., Goldstein, R. M., Gabriel, A., and Werner, C. L., 1994, On the derivation of coseismic displacement fields using differential radar interferometry: The Landers earthquake: Journal of Geophysical Research, v. 99, p. 19617–19634.

Zebker, H. A., Rosen, P. A., and Hensley, S., 1997, Atmospheric effects in interferometric synthetic aperture radar surface deformation and topographic maps: Journal of Geophysical Research, v. 102, p. 7547–7563.

Manuscript received October 24, 1997
Revised manuscript received March 2, 1998
Manuscript accepted March 24, 1998